情報計測処理論
「太陽系探査データ処理」
Analysis of solar system exploration data

新領域創成科学研究科　複雑理工学専攻
今村 剛　Takeshi Imamura

Recent remote-sensing orbiter missions

Venus Express

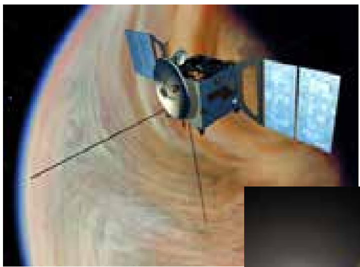

Mars Reconnaissance Orbiter

JUNO

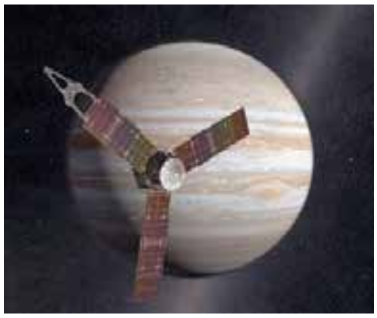

Akatsuki

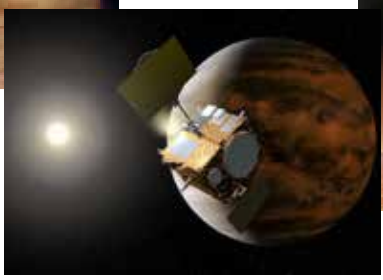

ExoMars Trace Gas Orbiter

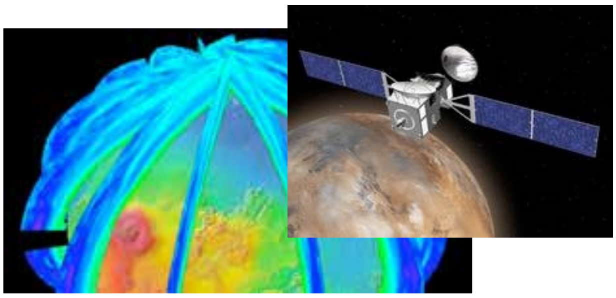

MMX

JUICE

Remote sensing in planetary exploration

- Radio wave measurement
  - Doppler measurement of spacecraft signals
  - Spectroscopy
  - Radar sounding
  - Radio interferometry (e.g, SAR, VLBI)

- Optical (short wavelength EM wave) measurement
  - Imagery
  - Spectroscopy
  - Laser sounding

Radio occultation measurement

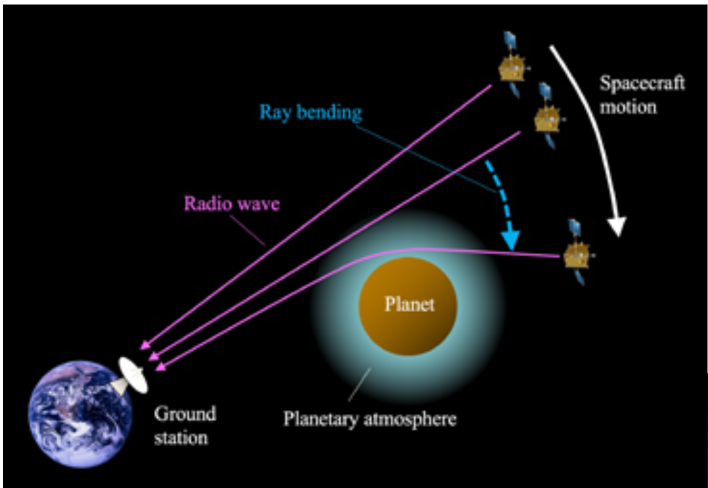

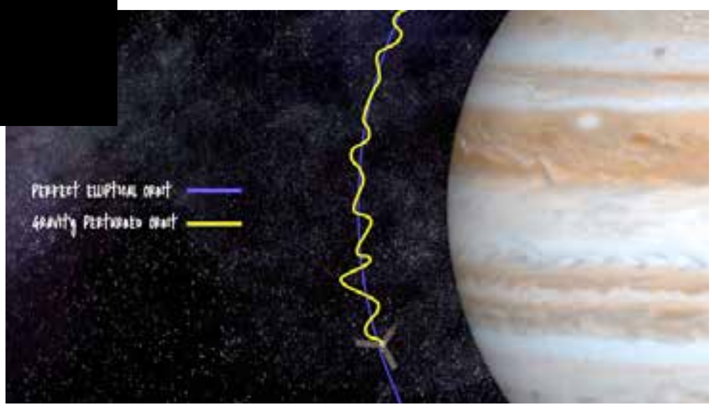

Observation of gravity anomaly by Doppler tracking of spacecraft (NASA's Juno)

Vertical temperature profiles of planetary atmospheres

(Mueller-Wodarg et al.)

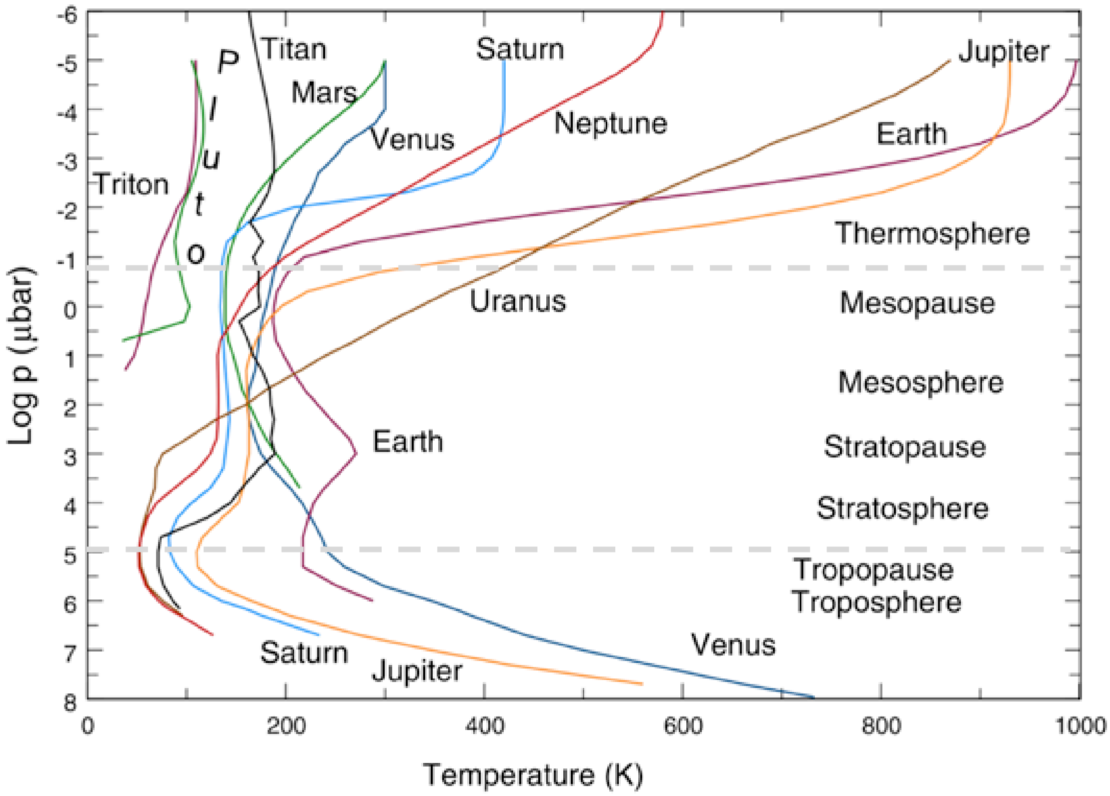

Radio occultation measurement

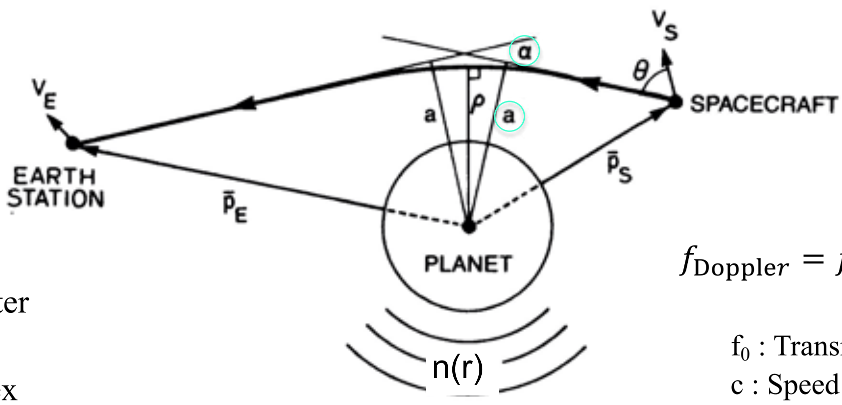

Tyler (1987)

$$f_{\text{Doppler}} = f_0 \frac{V_S \cos\theta}{c}$$

f_0 : Transmit frequency
c : Speed of light

a : Impact parameter
α : Bending angle
n : Refractive index
r : Distance from planet center

Abel transformation:

$$\ln n(r) = -\frac{1}{\pi}\int_{a_1}^{\infty} \ln\left\{\frac{a}{a_1} + \left[\left(\frac{a}{a_1}\right)^2 - 1\right]^{\frac{1}{2}}\right\} \frac{d\alpha}{da} da$$

$n(r)\, r = a$ $\qquad$ a : Impact parameter for a ray whose radius of closest approach is r

Refractive index n is related to atmospheric structure:

$$\mu(r) = (n(r) - 1) \times 10^6$$
$$= \underbrace{\boxed{\kappa N_n(r)}}_{\text{neutral atmosphere}} - \underbrace{\boxed{40.3 \frac{N_e(r)}{f_0^2} \times 10^6}}_{\text{plasma}}$$

μ : Refractivity

N_n : Neutral number density

N_e : Electron number density

Neutral atmosphere's temperature based on hydrostatic equilibrium:

$$T(r) = \frac{N_n(r_{top})}{N_n(r)} T(r_{top}) + \frac{\overline{m}}{kN_n(r)} \int_r^{r_{top}} N_n(r')g(r')dr$$

- Temperature at the upper boundary should be given from empirical models. The effect of the upper boundary almost disappears 1-2 scale heights below the boundary.

Hydrostatic equilibrium

The balance between the pressure gradient force and the gravitational acceleration in the vertical direction is

$$-S\Delta p = g\rho S\Delta z$$

$$\therefore \frac{dp}{dz} = -g\rho \qquad (1.1)$$

g : gravitational acceleration p : pressure
z : altitude ρ : mass density (kg/m^3)

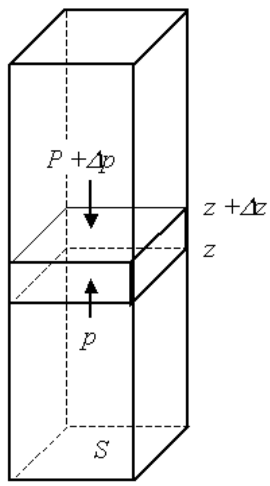

Integrating (1.1) we have

$$p(z) = \int_z^\infty g\rho(z')dz'$$

The equation of state:

$$p = \rho RT$$

R : gas constant (= 287 J/K/kg for Earth)
$R = k/m$, where k is Boltzmann's constant and m is the mean mass of molecules

Retrieval of a temperature profile

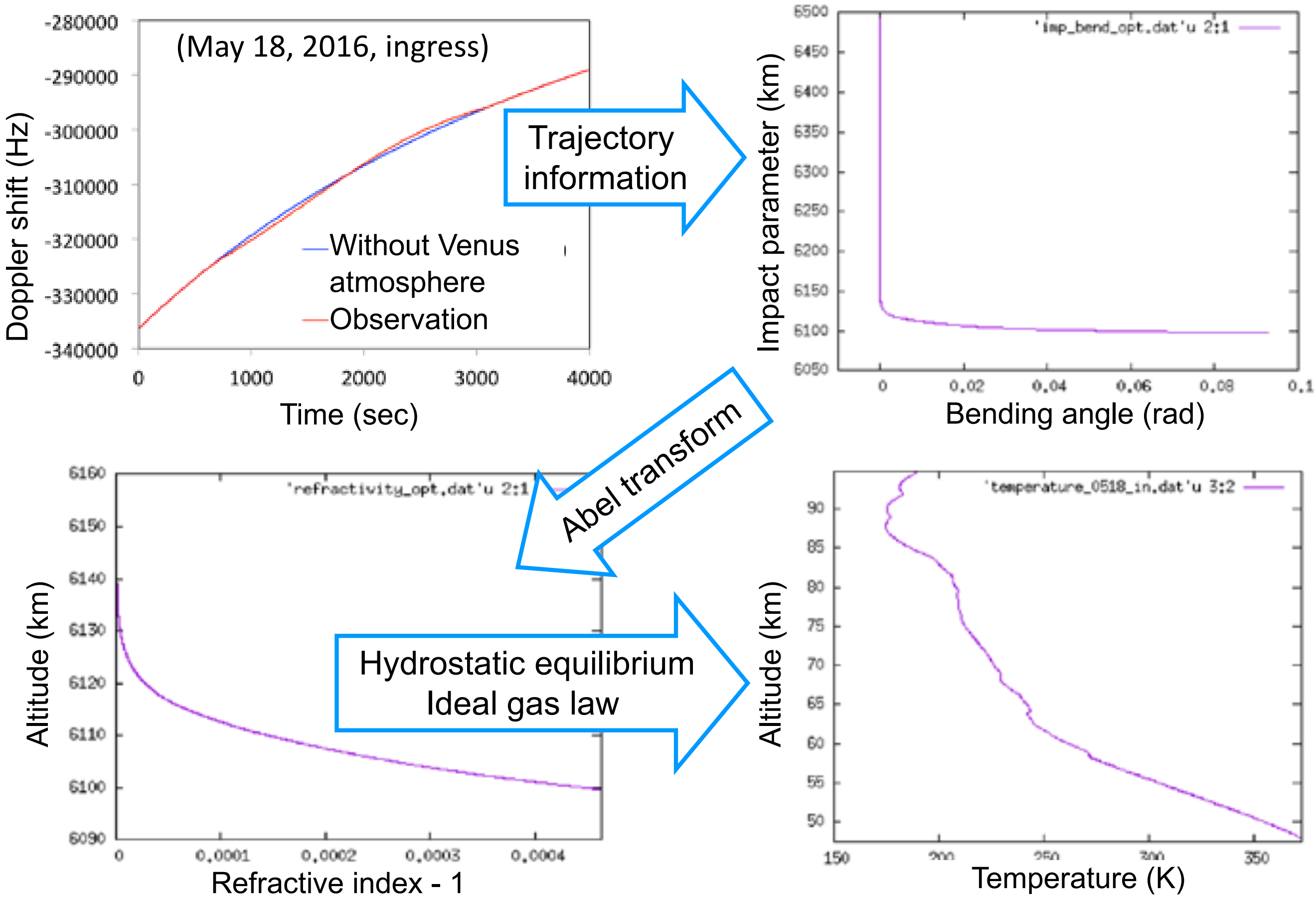

Required accuracy

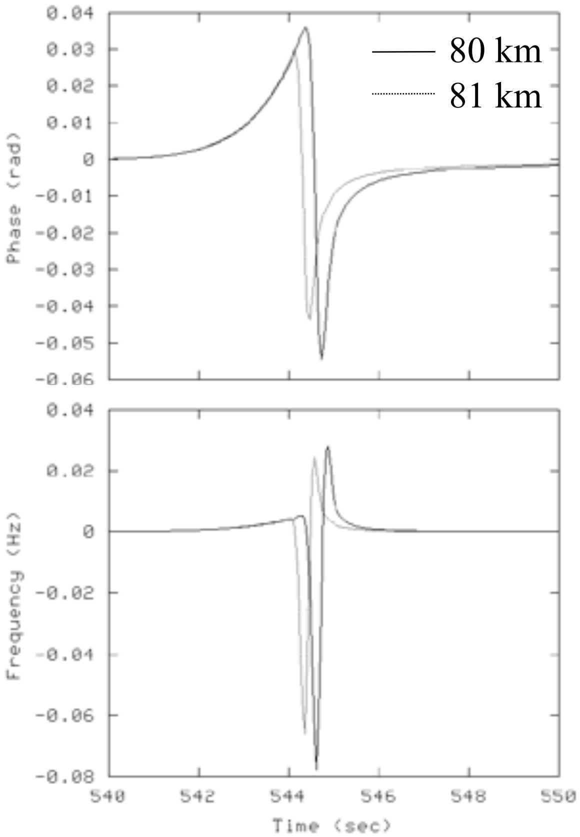

Change in phase/frequency caused by a Gaussian-type 0.2 K-perturbation with 1 km-thickness

Transmit frequency ~ 8 GHz

Required frequency accuracy ~ 0.02 Hz

→ **Required frequency stability** ~ 2×10^{-12}

Phase accuracy $\sigma_{rad} = 0.01$ rad

→ **Required S/N ratio** = $1/\sigma_{rad}^2 = 10000$

Allan variance, Allan deviation

Allan variance

$$\sigma_y^2(\tau) = \frac{1}{2}\left\langle (\bar{y}_{n+1} - \bar{y}_n)^2 \right\rangle$$

$$\bar{y}_n = \frac{f_n}{f_0}$$

: n-th fractional frequency average over the observation time τ
(f_n : n-th measurement of frequency
f_0 : Nominal frequency)

Allan deviation

$$\sigma_y(\tau) = \sqrt{\sigma_y^2(\tau)}$$

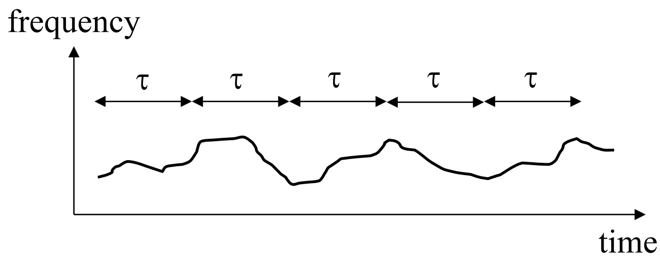

Ultra-Stable Oscillator (USO) on Venus orbiter Akatsuki

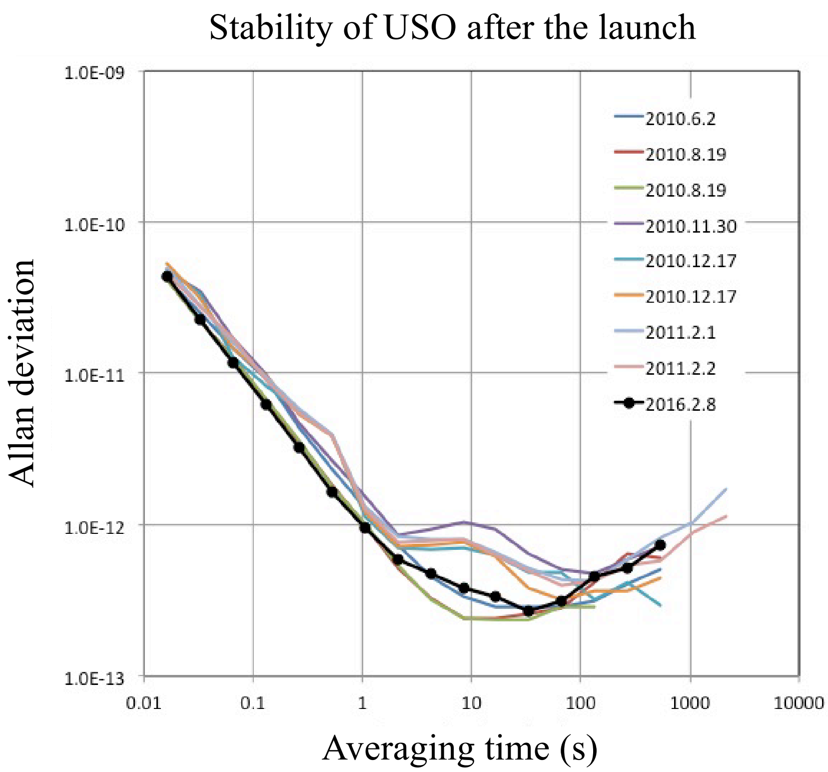

USO on Akatsuki

The requirement (Allan dev < 1×10^{-12} for τ = 1-1000 s) is satisfied.

Data acquisition

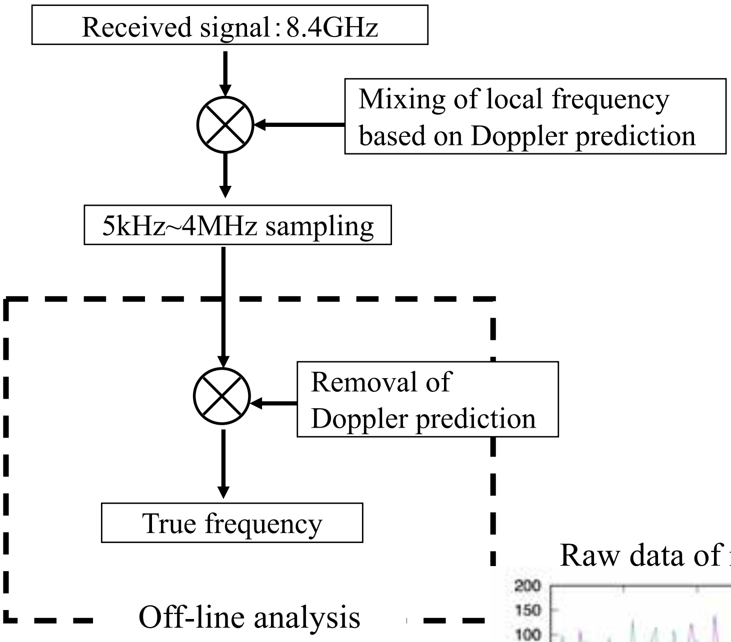

Usuda Deep Space Center (UDSC)

Raw data of radio wave from Venus orbiter Akatsuki

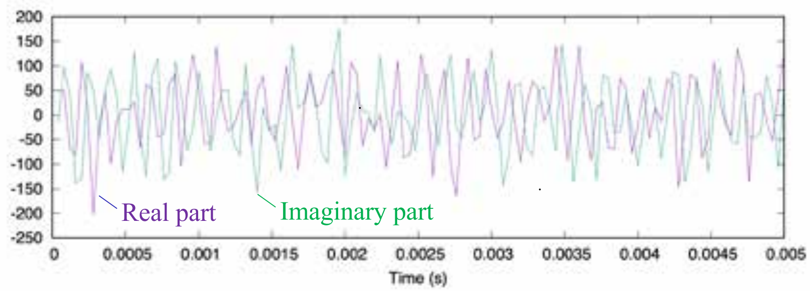

Need for narrow-band filtering (example from Akatsuki)

- Signal level at the receiver: $P = 3.0 \times 10^{-17}$ W (at 1.73 × Earth-Sun-distance)
- Noise temperature of the receiver = 96 K (Usuda Deep Space Center)

  → $kT \sim 1.3 \times 10^{-21}$ (unit: J = W/Hz)

Letting the band width be B (Hz), the S/N ratio is given by

$$P / kTB \sim 2.3 \times 10^{-4} / B$$

So that the S/N ratio is higher than the required value of ~10000, we require

$$B < 20 \text{ Hz}$$

→Time resolution ~ 0.05 s : Acceptable

Signal spectrum

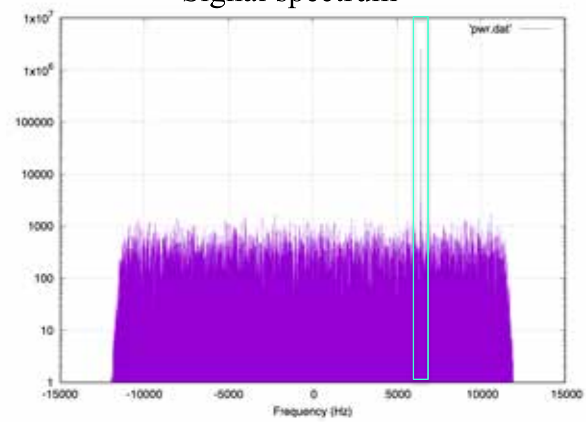

Usually the influence of the uncertainty in the orbital motion the transmit frequency is larger than this bandwidth. We must first stabilize the signal frequency.

Rough estimation of frequency

Successive FFTs for short segments

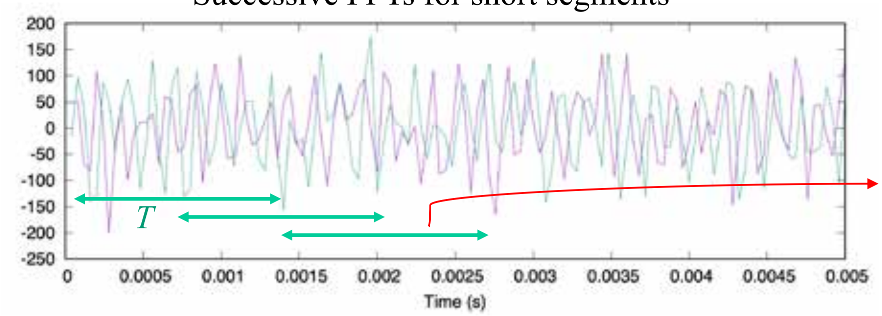

Fitting of Sinc function

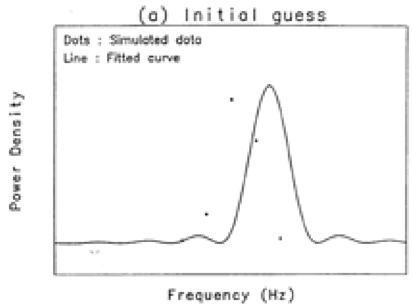

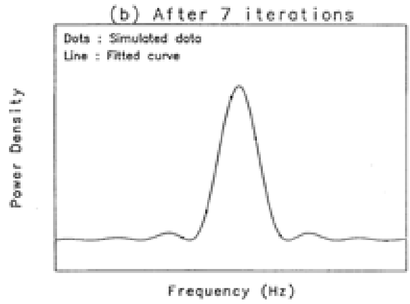

Frequency resolution of FFT

$$\Delta f = 1/T$$
$$= B/N$$

T : Time length of FFT
N : FFT length
B : Bandwidth = sampling frequency (for complex data)

For example, to achieve a frequency accuracy of $\Delta f < 0.1$ Hz, the time length should be $T = 1/\Delta f > 10$ s.

Rough estimation of frequency

Successive FFTs for short segments

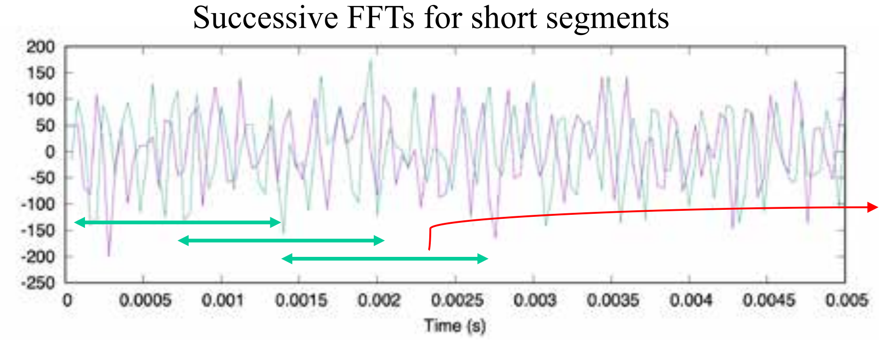

Fitting of Sinc function

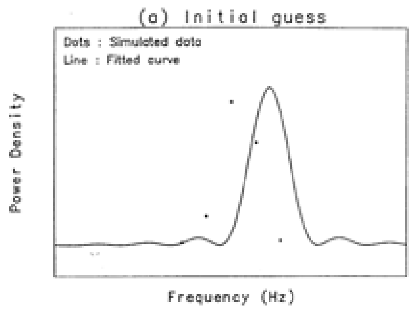

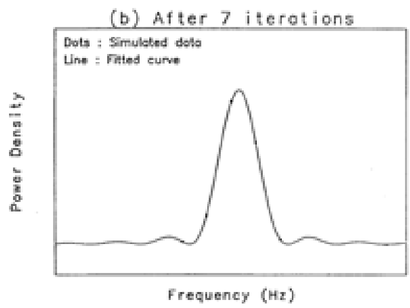

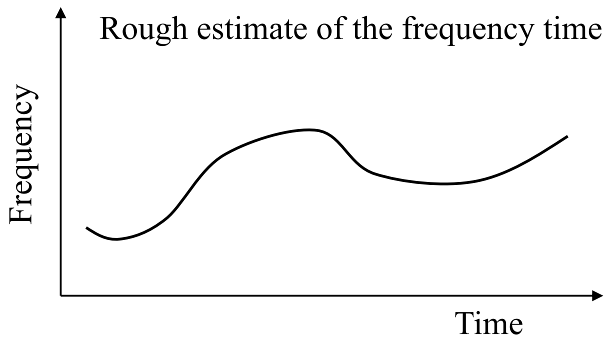

Extracting the roughly estimated frequency

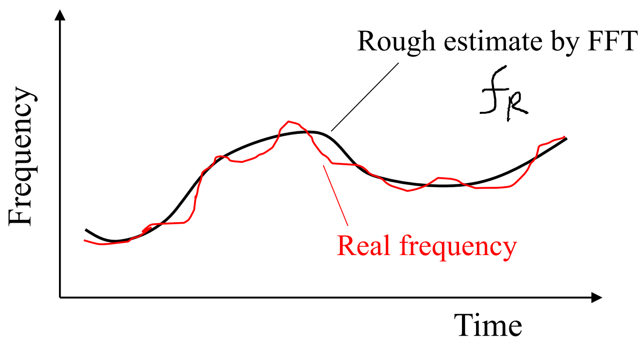

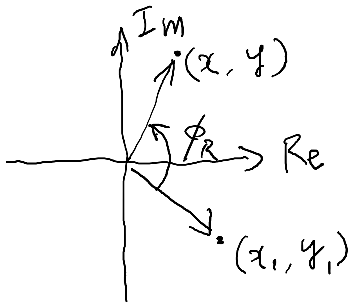

$$\phi_R = \int^t f_R(t')\, dt'$$

$$\begin{pmatrix} x_1(t) \\ y_1(t) \end{pmatrix} = \begin{pmatrix} \cos(-\phi_R) & -\sin(-\phi_R) \\ \sin(-\phi_R) & \cos(-\phi_R) \end{pmatrix} \begin{pmatrix} x(t) \\ y(t) \end{pmatrix}$$

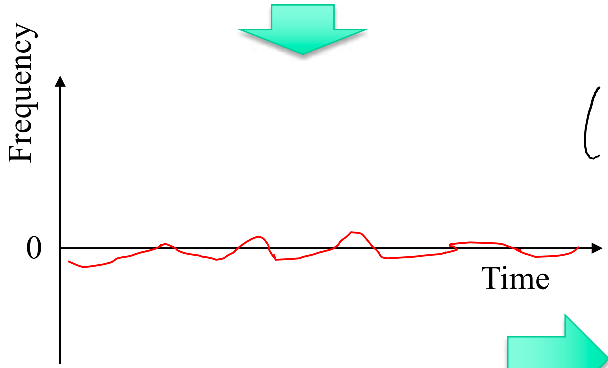

Narrow-band filtering

Filtering and decimation

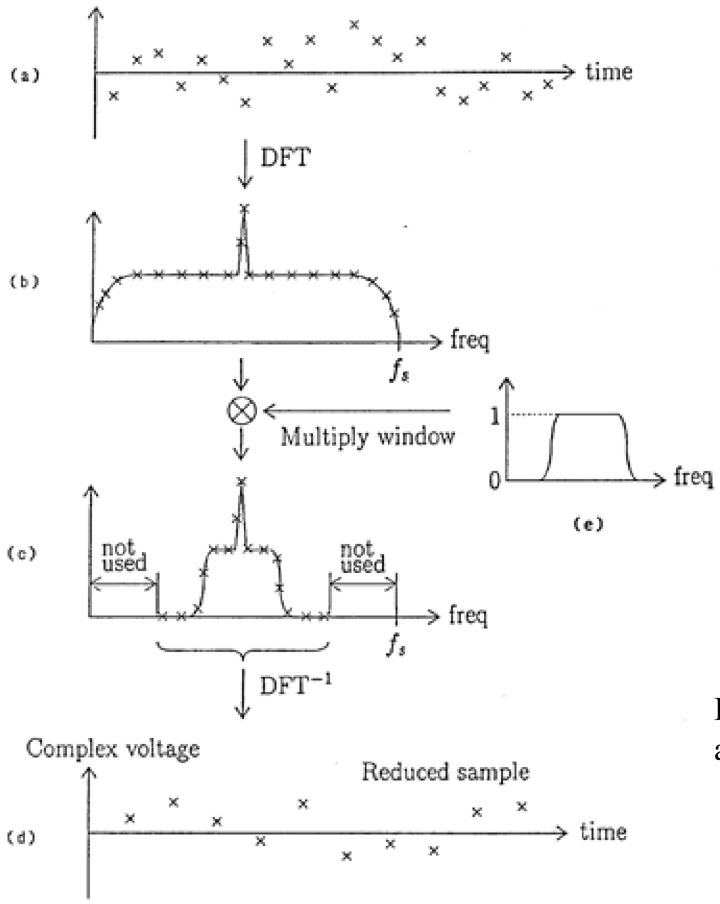

Low-noise data is created by arrow-band filtering

Precise phase/frequency estimation by phase unwrapping

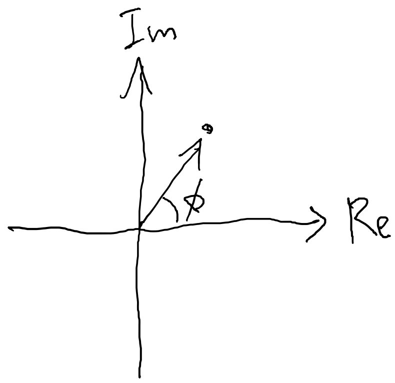

$$f = \frac{d\phi}{dt}$$

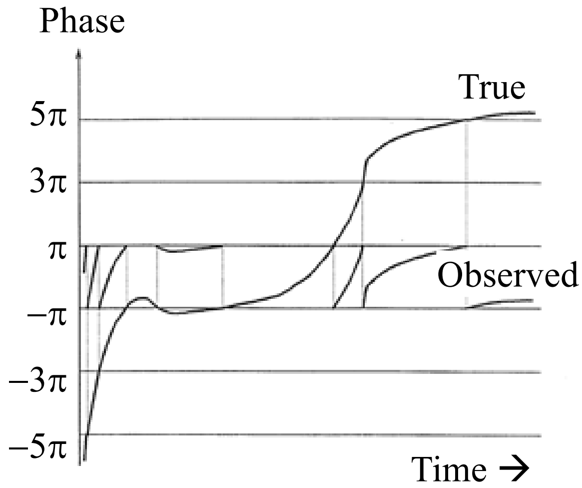

With sufficiently low-noise, the phase can be obtained from the real and imaginary components of the data at each time step.
The frequency is obtained by differentiating the phase.

Temperature profiles of the Venus atmosphere obtained by Akatsuki radio occultation

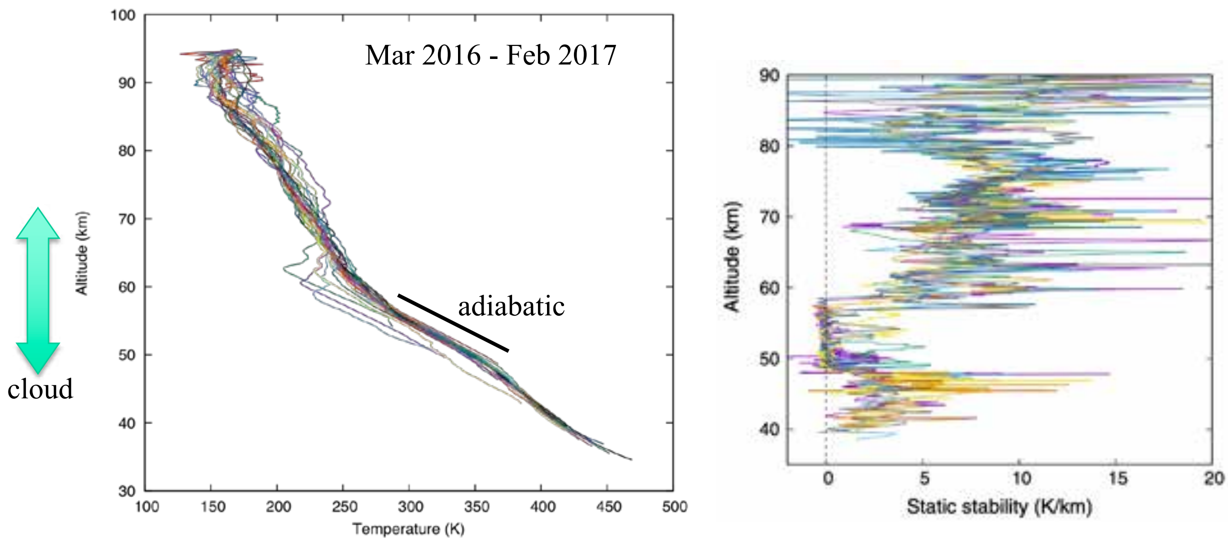

Imamura et al. 2017

Static stability: $$S = \frac{dT}{dz} - \frac{g}{c_p}$$

T : temperature
z : altitude
g : gravitational acceleration
c_p : specific heat for constant pressure

Latitude-altitude cross sections

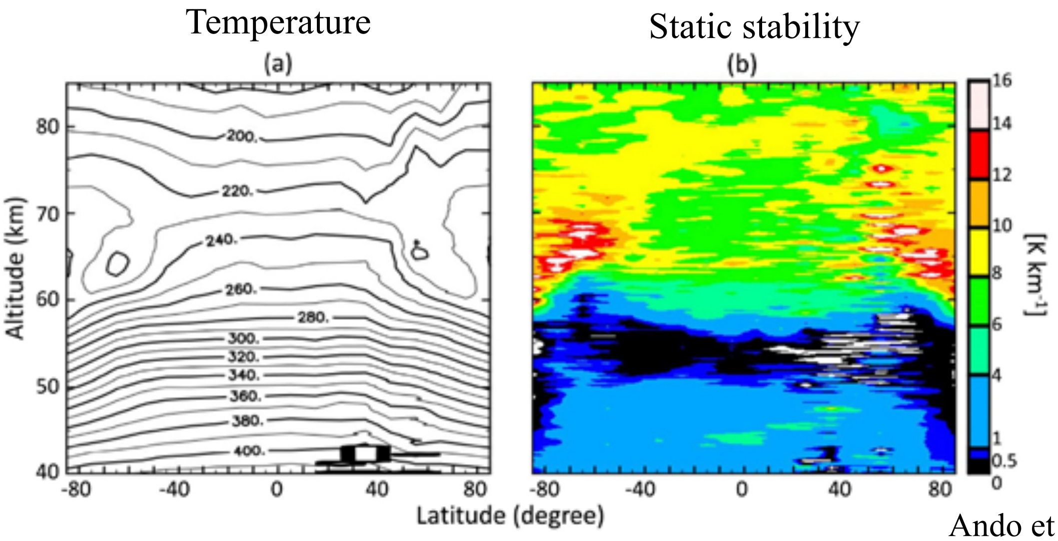

Ando et al. (2020)

Figure 2. Latitude–height distributions of zonally and temporally averaged (**a**) temperatures and (**b**) static stability obtained from Venus Express and Akatsuki radio occultation measurements.

- Near-neutral layer extends to the sub-cloud region in the high latitude
- Unknow energy transport below clouds ?

limitation of vertical resolution

$$F_n = \sqrt{\frac{n\lambda d_1 d_2}{d_1 + d_2}}, \quad d_1, d_2 \gg n\lambda,$$ [3]

where

F_n is the nth Fresnel zone radius,
d_1 is the distance of P from one end,
d_2 is the distance of P from the other end,
λ is the wavelength of the transmitted signal.

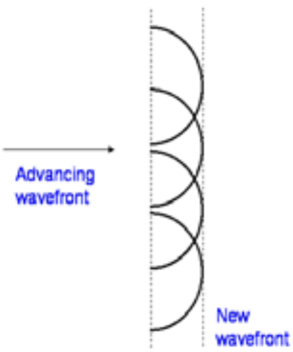

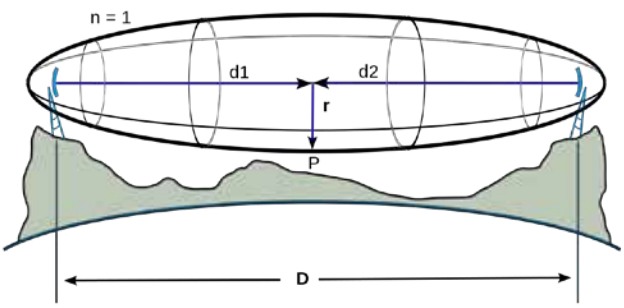

(Wikipedia)

n = 1 : First Fresnel zone. Outside this zone a destructive inference greatly reduces the contribution to the received signal.

F_1 is typically several hundred kilometers for interplanetary missions.

Examples of Venus' electron density profile from Akatsuki radio occultation

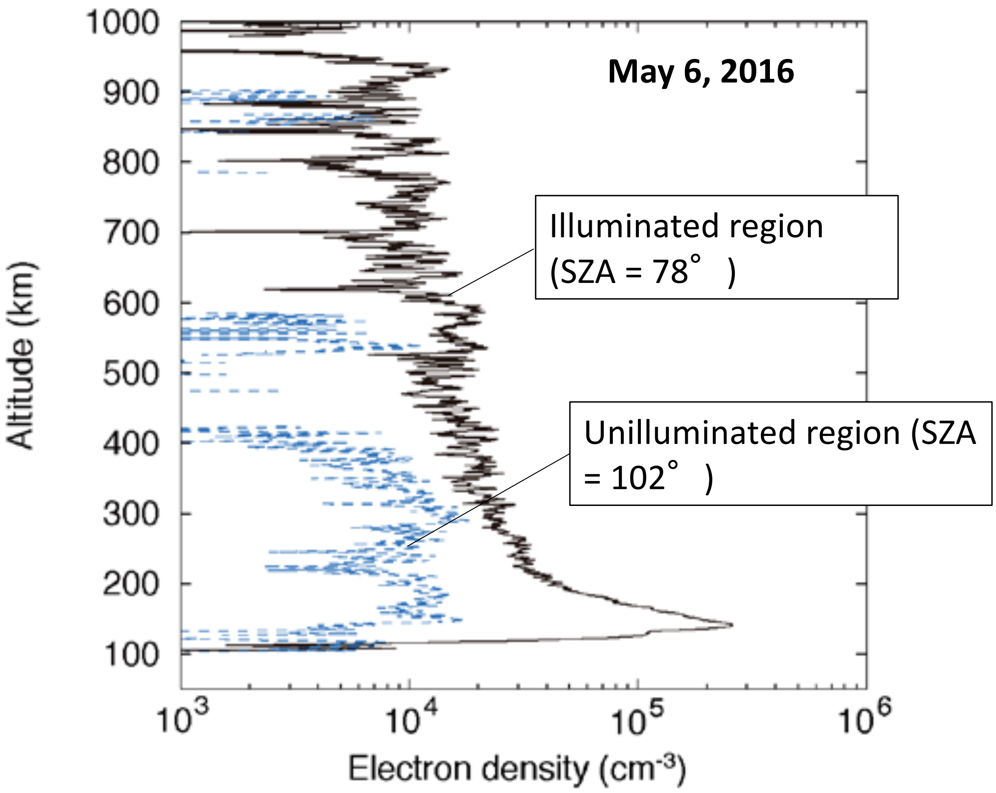

Radio occultation of lunar photoelectron layer with SELENE

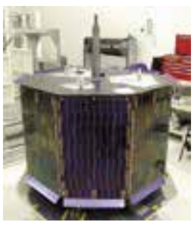

Vstar subsatellite

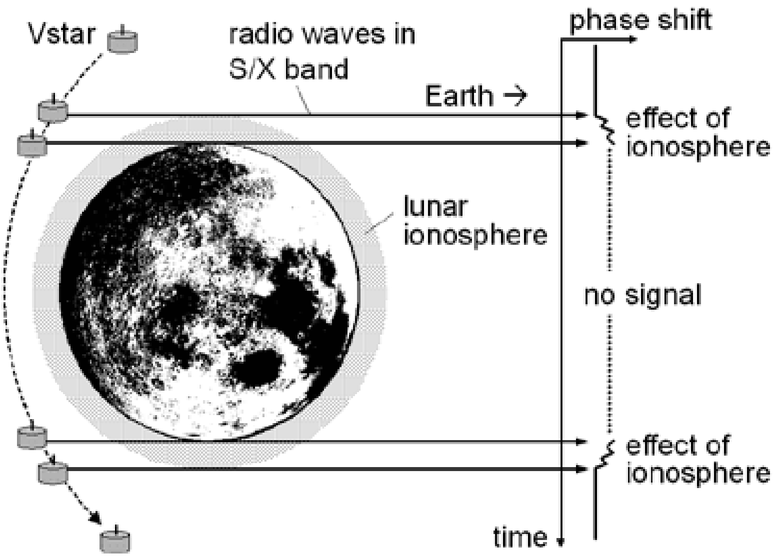

Usuda Deep Space Center, Japan

Dual-frequency method for precise plasma measurement

To remove the effect of the fluctuation of the transmitted signal's frequency and the neutral atmosphere's contribution, two frequencies generated from the common onboard oscillator are used. A linear combination of these phases can extract the plasma contribution.

$$\Delta\phi_S = -\frac{40.3}{c\, f_S} N_e + \alpha\, f_S$$: Phase shift of S-band (2.3 GHz)

$$\Delta\phi_X = -\frac{40.3}{c\, f_X} N_e + \alpha\, f_X$$: Phase shift of X-band (8.4 GHz)

$$\delta\phi = \Delta\phi_S - \frac{f_S}{f_X}\Delta\phi_X = -\frac{40.3}{c} f_S \left(\frac{1}{f_S^2} - \frac{1}{f_X^2} \right) \cdot N_e$$: Differential phase

N_e : Column electron density
f_S : S-band frequency
f_X : X-band frequency

Example from lunar plasma layer measurement in SELENE mission

Phase deviation in S-band (ϕ_S) and X-band (ϕ_X)

Differential phase $\phi_{diff} = \phi_S - f_s/f_x\, \phi_X$
(f_s, f_x : S/X-band nominal freq.)

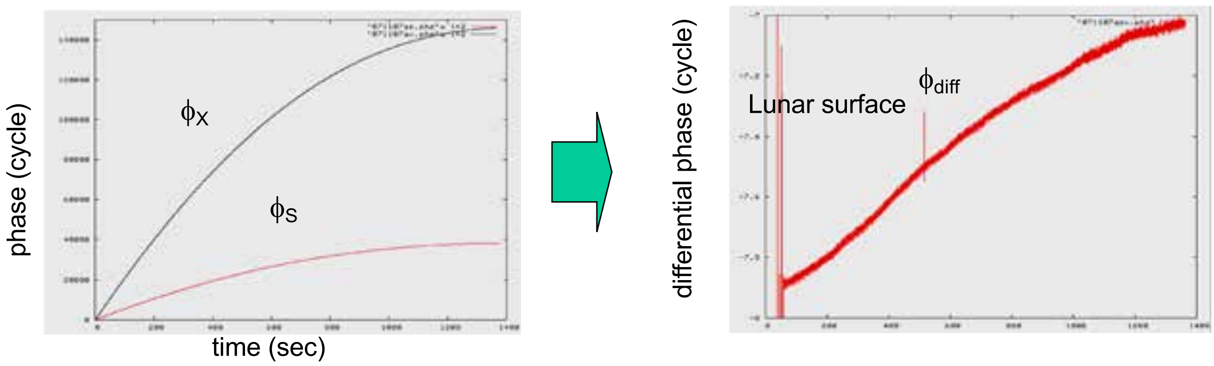

ϕ_{diff} is proportional to the electron density integrated along the ray path.

Mean density profile of lunar ionosphere at SZA<60°

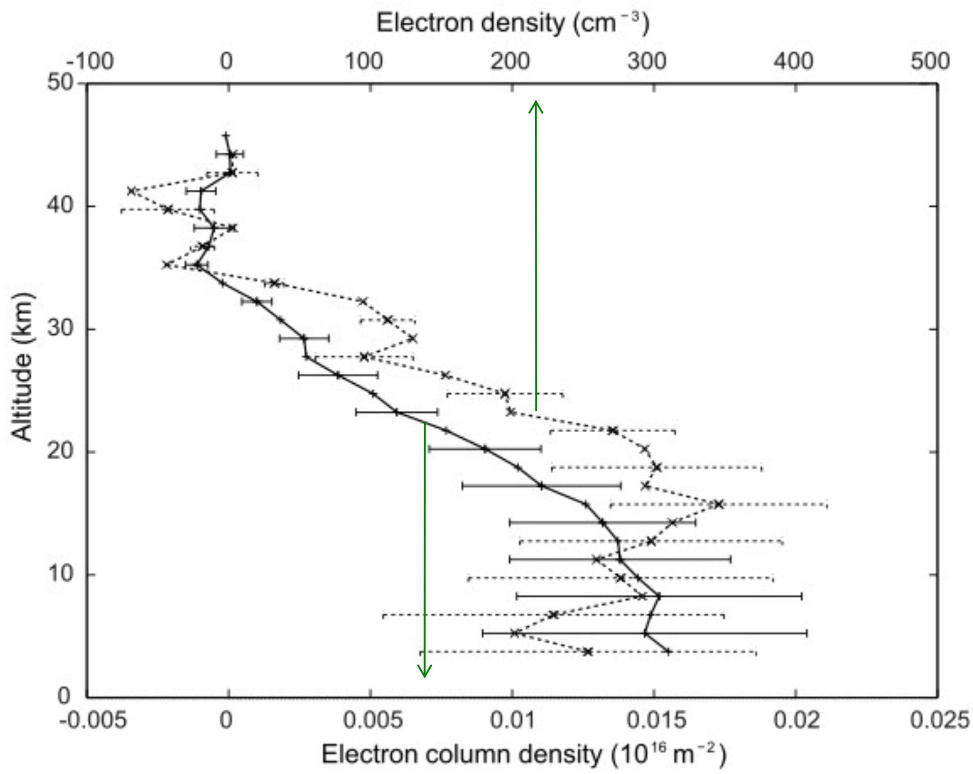

Imamura et al. (2012)

GPS radio occultation for Earth

UCAR/COSMIC homepage

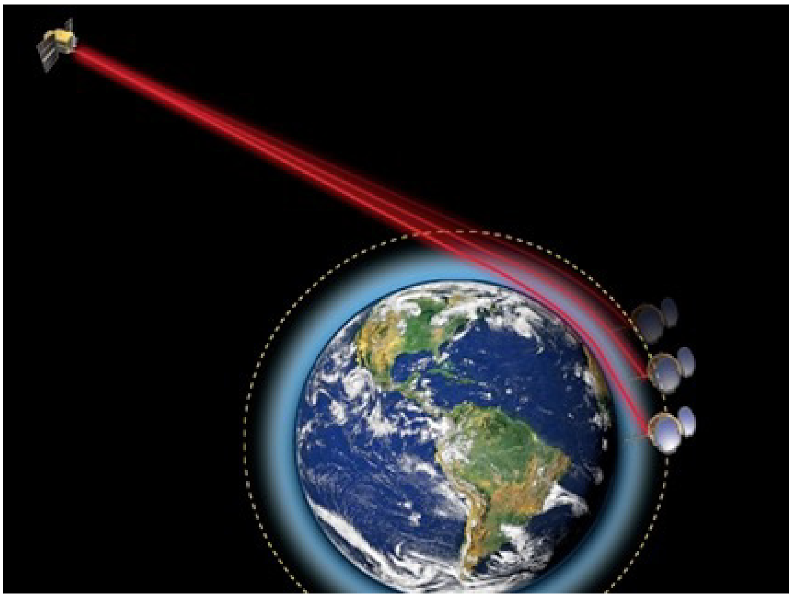

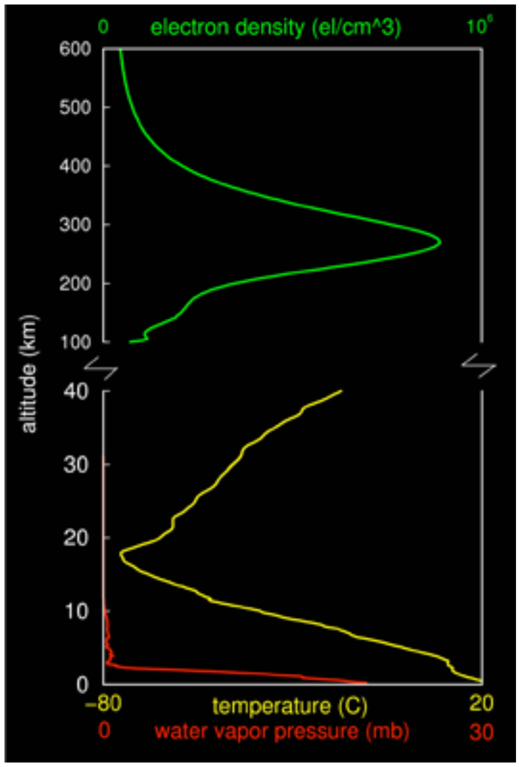

COSMIC : Constellation Observing System for Meteorology, Ionosphere, and Climate

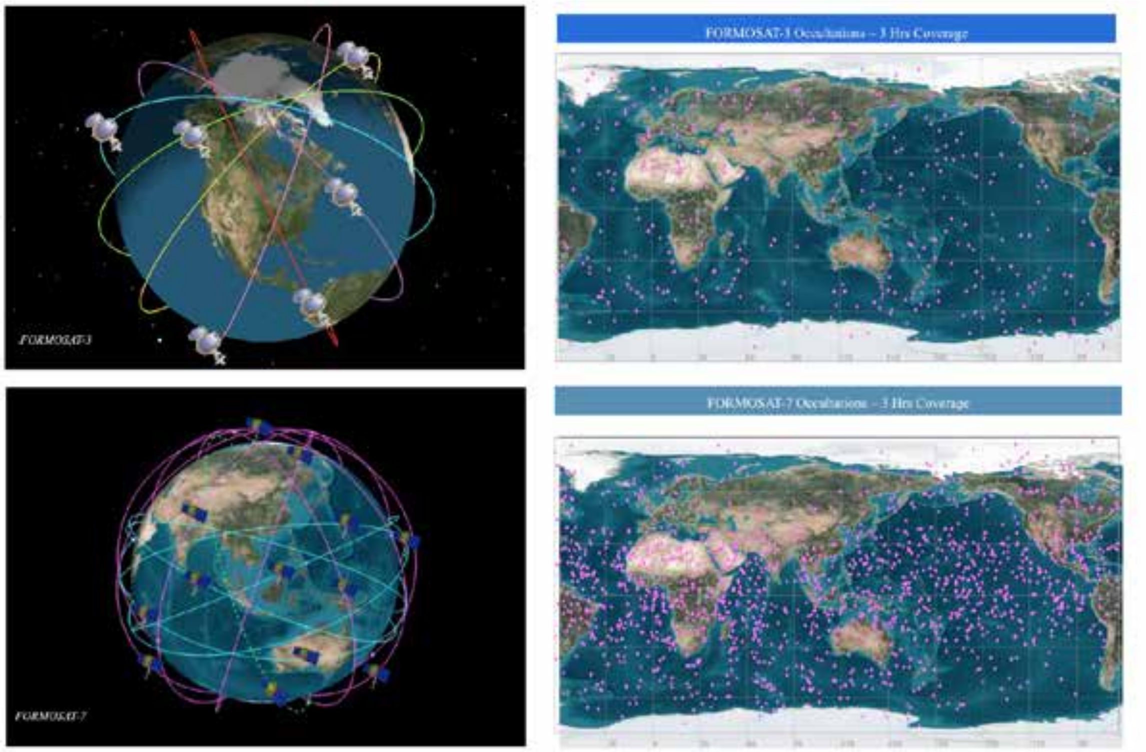

UCAR/COSMIC homepage

Fig. 1. Constellation design and estimated distribution of GPS RO soundings over a 3-h period from COSMIC/FORMOSAT-3 and COSMIC-2/FORMOSAT-7. The first tropical constellation of COSMIC-2 will be launched in 2016, and the second constellation will be launched in 2018. COSMIC-2 will provide an order of magnitude more GPS RO soundings over the tropics, which will have a significant impact on tropical cyclone prediction.

Doppler tracking of Juno spacecraft

- The spacecraft acts as a test particle falling in the gravity field of the planet. Jupiter’s gravity is inferred from range-rate measurements between a ground antenna and the spacecraft during perijove passes.
- The ground station transmits two carrier signals, at 7,153 MHz (X band) and 34,315 MHz (Ka band). On board, an X-band transponder and a Ka-band frequency translator lock the incoming carrier signals and retransmit them back to the ground station at 8,404 MHz and 32,088 MHz, respectively. The range-rate (Doppler) observable is obtained by comparing the transmitted and received frequencies.
- Spherical harmonics representation of planetary gravity fields is determined by the density distribution inside the body.

Doppler tracking of Juno spacecraft

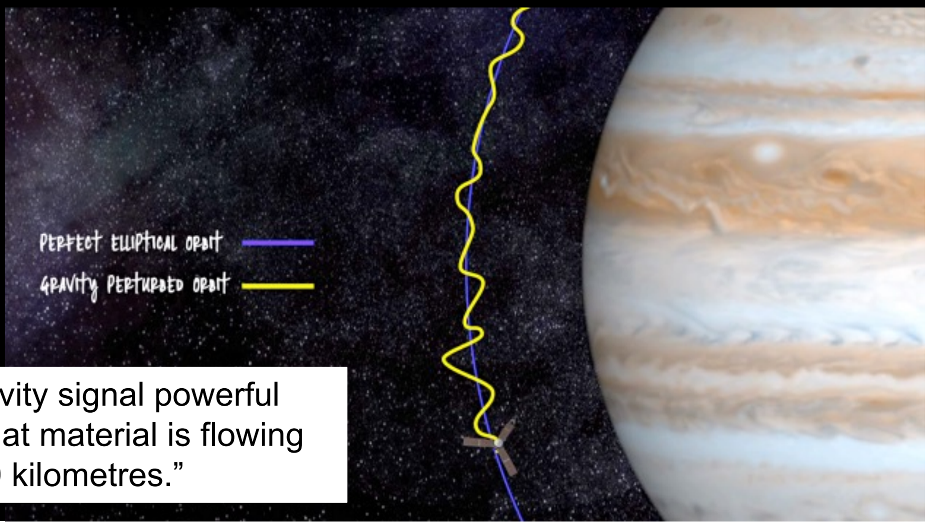

"Juno detected a gravity signal powerful enough to indicate that material is flowing as far down as 3,000 kilometres."

Less et al. (2018)

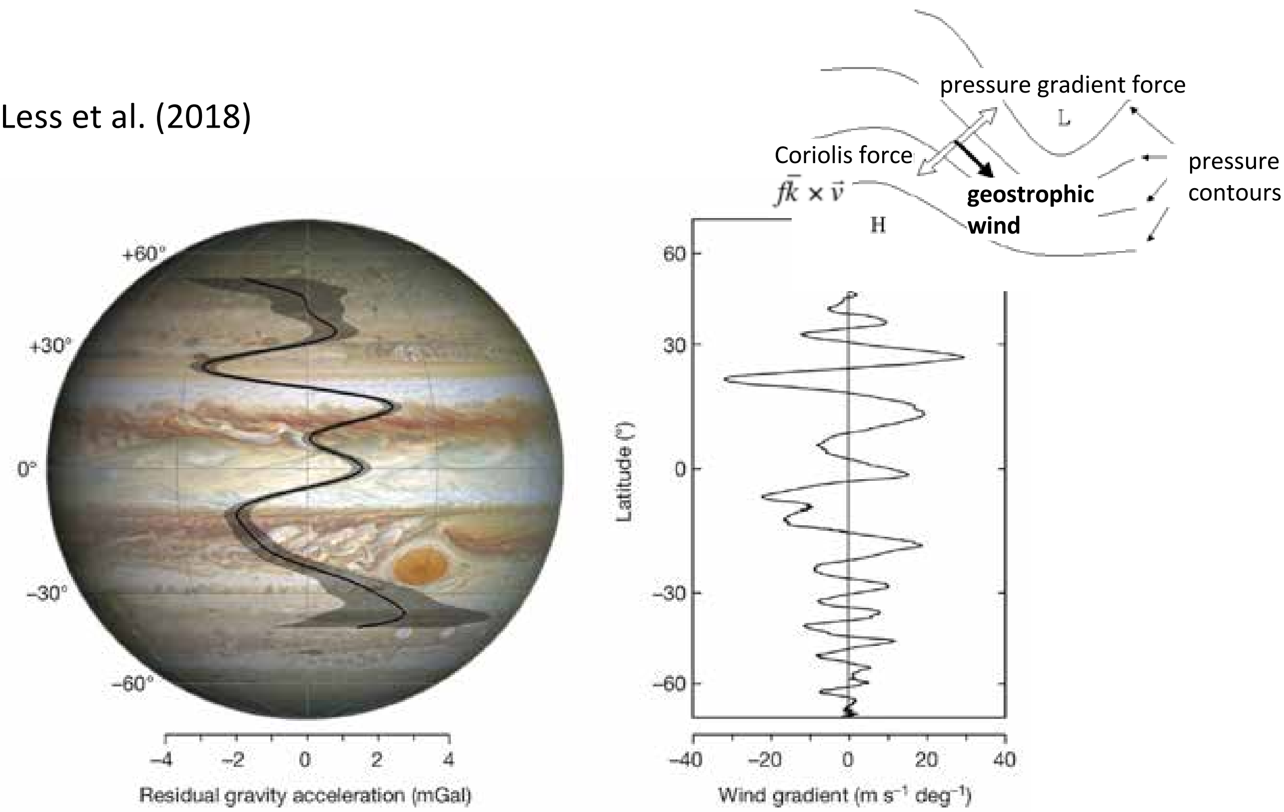

"The observed jet streams, as they appear at the cloud level, extend down to depths of thousands of kilometres beneath the cloud level, probably to the region of magnetic dissipation at a depth of about 3,000 kilometres"

Deep models: Taylor–Proudman theorem

- In a fluid that is steadily rotated, the fluid velocity will be uniform along any line parallel to the axis of rotation.

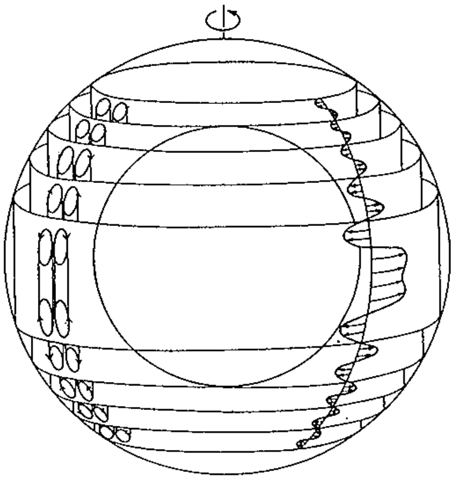

Busse (1994)

Momentum equation in rotational frame

$$\frac{d\vec{v}}{dt} + 2\vec{\Omega} \times \vec{v} + \frac{1}{\rho}\nabla p + \nabla\Phi = 0$$

Assuming non-compressivity and d/dt=0, the curl is applied to give

$$\vec{\Omega} \cdot \nabla\vec{v} = 0$$

Taking z-axis along the planet's rotational axis,

$$\frac{\partial\vec{v}}{\partial z} = 0$$

Planetary images

- The contrast in an original image is dominated by geometrical (illumination) effects. To visualize the detail of the surface, the effects need to be removed.

UV image of Venus taken by Akatsuki

Photometric correction

- The incident solar flux at each position on the planetary surface is proportional to the cosine of the incidence angle.
- The illumination effect can be roughly removed by dividing the original image by the model image, which is cosine of the incidence angle. (In real applications, more complicated model is used.)

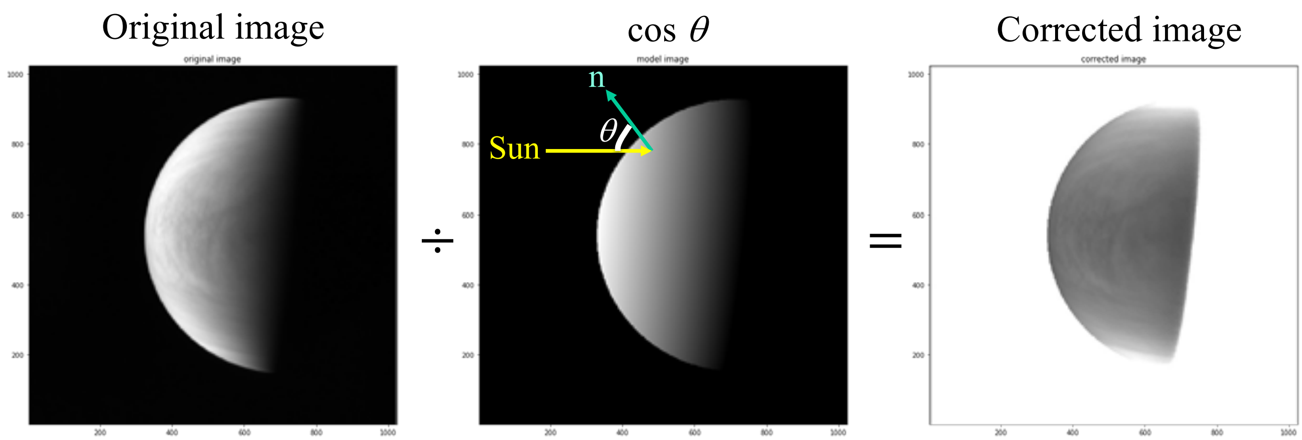

High-pass filtering

- To see the details of the surface, high-pass filtering is frequently used.
- High-pass filtering can be done by subtracting a smoothed image from the original (corrected) image. Moving average (running average) with a Gaussian function is frequently used for smoothing.

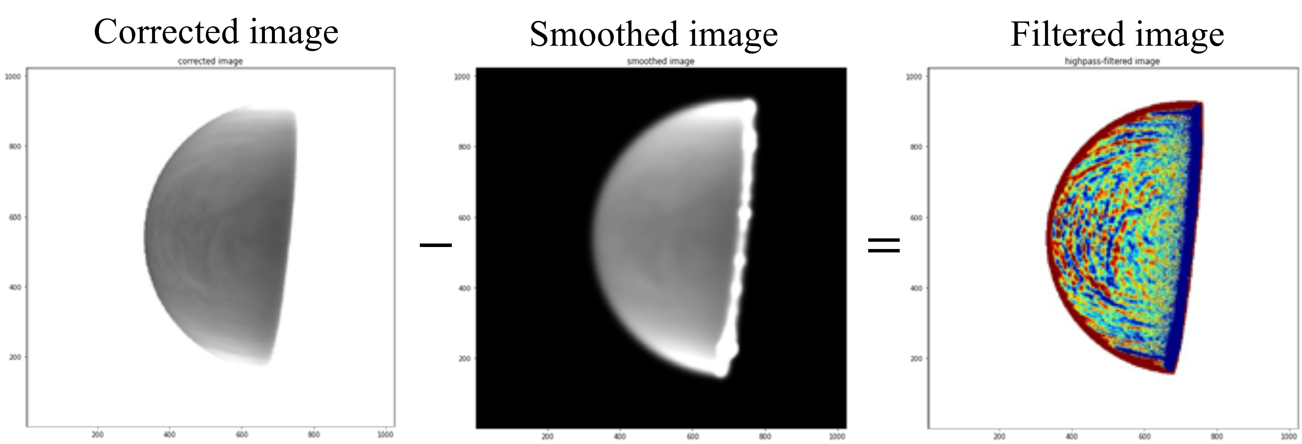

Ellipse fitting to precisely determine the camera pointing accuracy

- The accuracy of the pointing direction of onboard cameras measured by the spacecraft is insufficient in many cases.
- The pointing information can be corrected by fitting an ellipse to the limb of the planet.

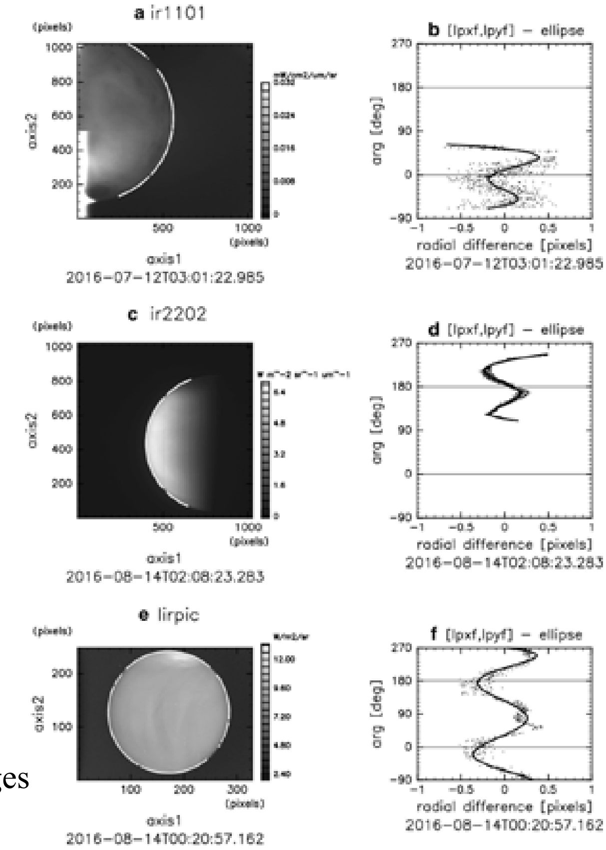

Ellipse fitting to Venus images (Ogohara et al. 2017)

Projection onto planetary coordinate

- Movement of the atmosphere can be observed by projecting successive images onto the planetary coordinate.

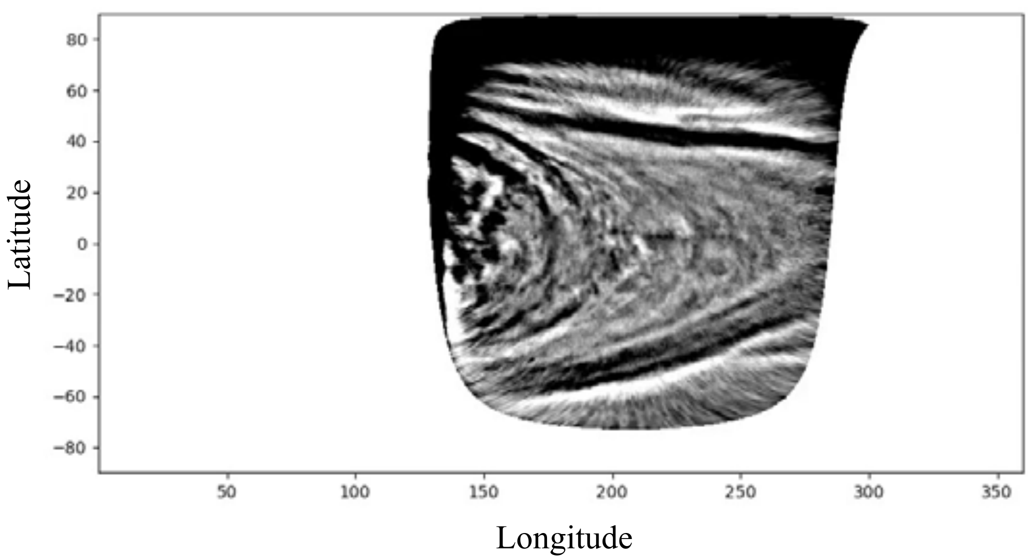

Cloud tracking with cross-correlation method

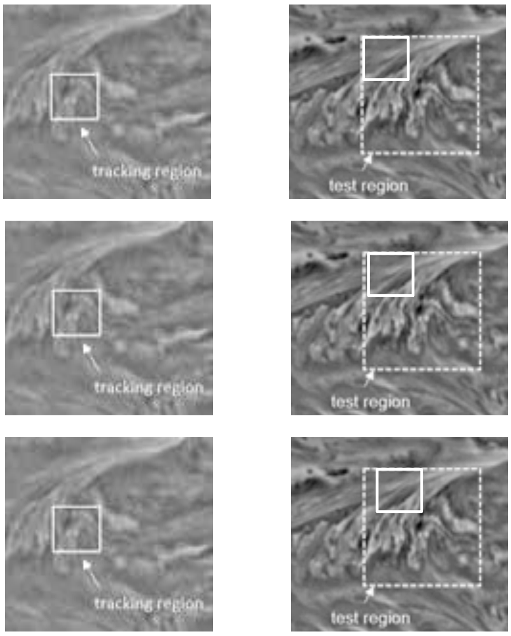

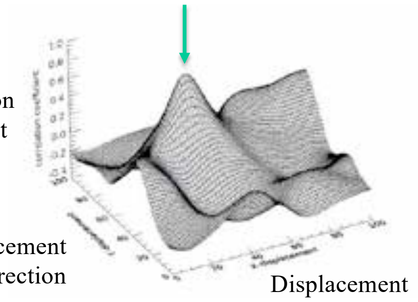

- The peak position on the correlation surface gives the displacement vector.
- Division the displacement by the time interval gives the velocity vector.

Cloud-tracked winds

Earth

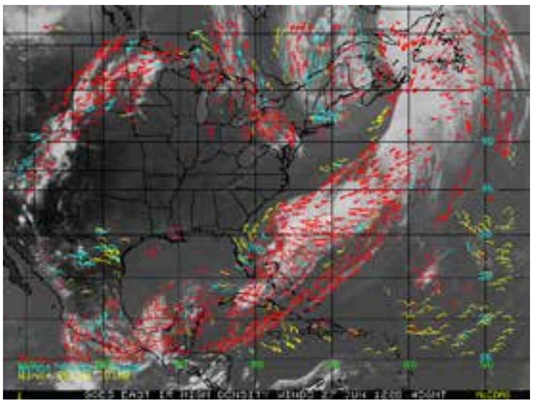

GOES winds derived from cloud and water vapor images (©NOAA)

Venus

Horinouchi et al. (2020)

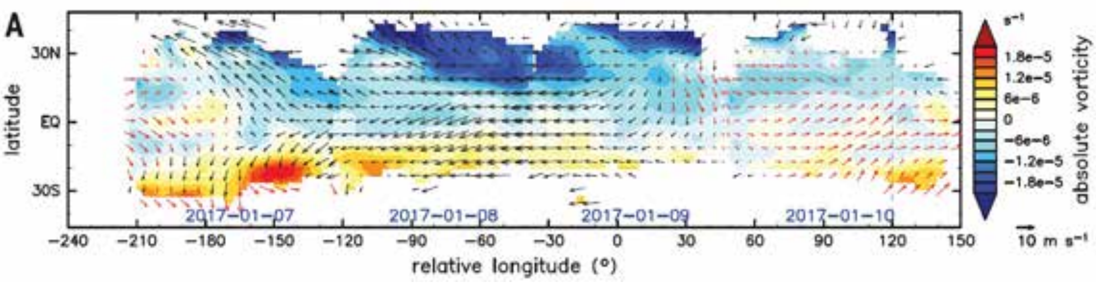

Superrotation of Venus' atmosphere

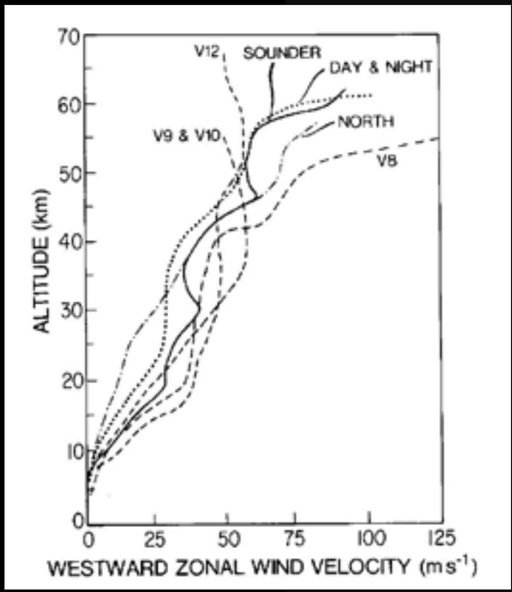

In-situ measurements of zonal winds (Schubert et al. 1980)

Zonal circulation at velocities 60 times faster than the solid surface

Maintenance of the superrotation by waves

Horizontal momentum transport

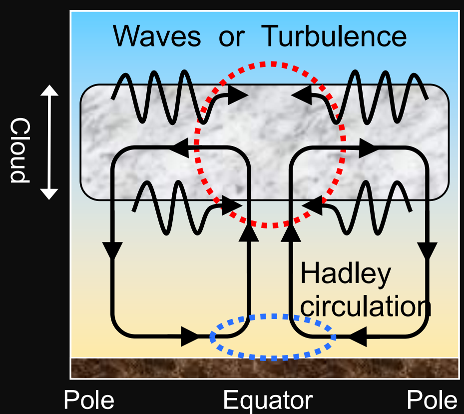

Vertical momentum transport

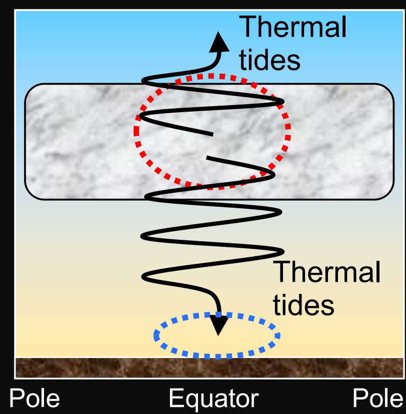

Acceleration

Deceleration

Tracking of faint cloud features in thermal infrared images of Venus

UV (283 nm) and thermal infrared (10 μm) images taken simultaneously by UVI and LIR (Fukuhara et al., 2017)

UV (283 nm)

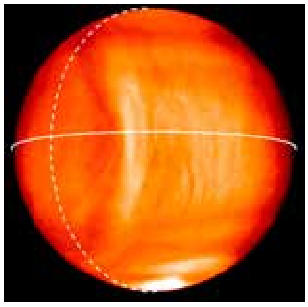

thermal infrared (10 μm)

Thermal infrared images allows observations of all local time regions

Characteristics of thermal infrared (LIR) data

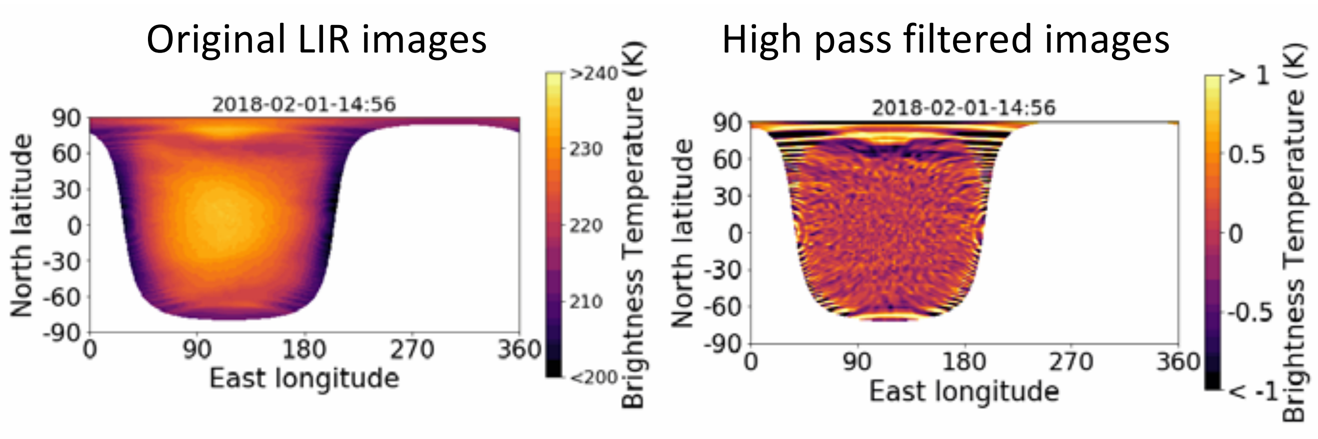

- Most of the small-scale cloud features have amplitudes comparable to or smaller than the LIR’s temperature resolution of 0.3 K.
- Difficult to track cloud patterns in original images

Noise reduction by averaging images

High-pass filtered map without averaging

Averaging images in a coordinate system moving with the background atmosphere

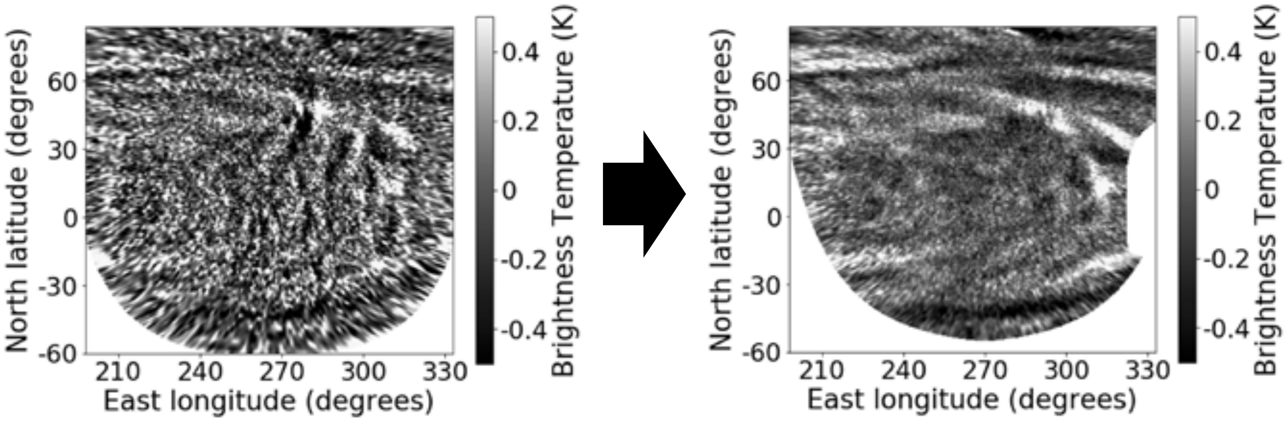

- Running-averaging of images in the time domain in a coordinate system moving with the superrotation
- S/N ratio is increased and topography-related features are smoothed out.

Moving features

Dayside

Nightside

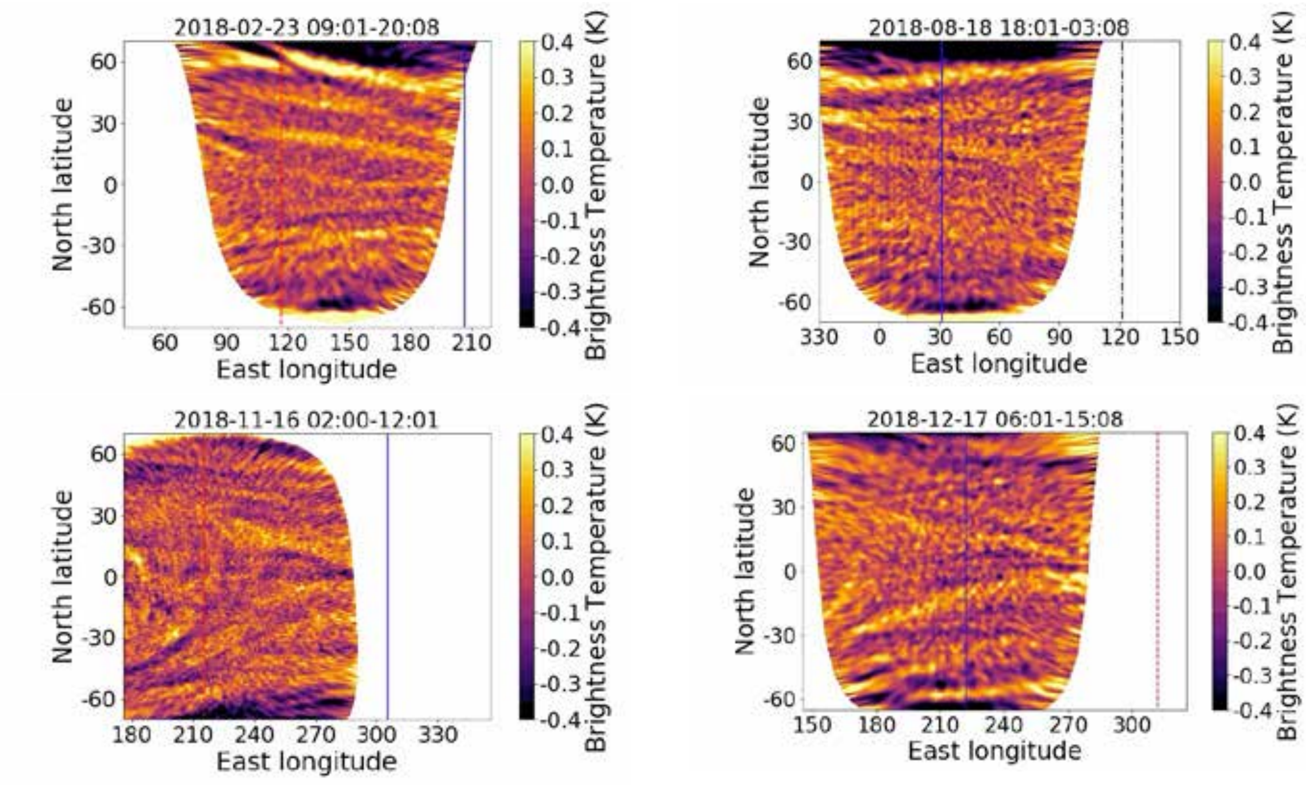

Local solar time-latitude distribution

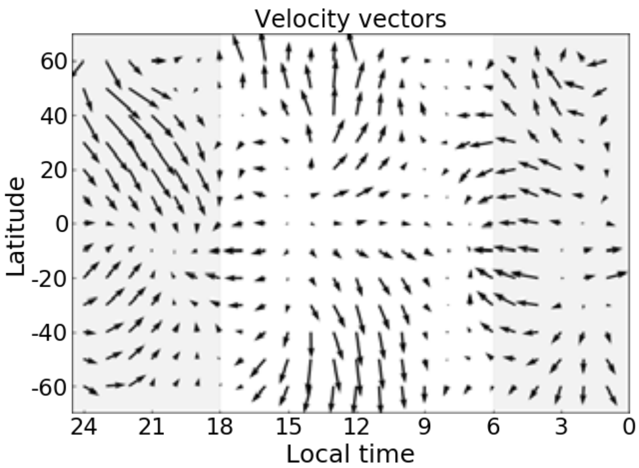

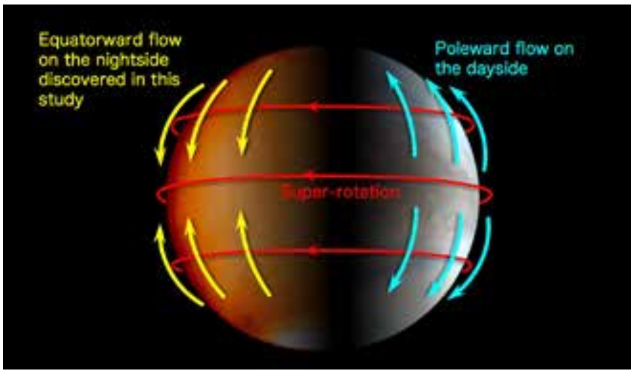

レポート課題

電波を用いた計測について一つ例を挙げて、その測定原理と応用例について1ページ以内で簡単に述べよ。

Give one example of measurement using radio waves and briefly describe its measurement principle and application in one page.

締切：7月31日

提出方法：ITC-LMSに提出